Highly Sensitive Single Domain Antibody–Quantum Dot Conjugates for Detection of HER2 Biomarker in Lung and Breast Cancer Cells

Tatsiana Y. Rakovich,[†,*] Omar K. Mahfoud,[†] Bashir M. Mohamed,[†] Adriele Prina-Mello,[†,‡] Kieran Crosbie-Staunton,[†] Tina Van Den Broeck,[⊥] Line De Kimpe,[⊥] Alyona Sukhanova,[∥,#,†] Daniel Baty,[▽] Aliaksandra Rakovich,[§] Stefan A. Maier,[§] Frauke Alves,[⊗] Frans Nauwelaers,[⊥] Igor Nabiev,[∥,#,†] Patrick Chames,[▽] and Yuri Volkov[†,‡]

[†]School of Medicine, Department of Clinical Medicine, Institute of Molecular Medicine, Trinity College, Dublin 8, Ireland, [‡]Centre for Research on Adaptive Nanostructures and Nanodevices, Trinity College, Dublin 2, Ireland, [§]Physics Department, Imperial College London, London SW7 2AZ, United Kingdom, [⊥]BD Biosciences, Erembodegem-Dorp 86, B-9320 Erembodegem, Belgium, [∥]Laboratoire de Recherche en Nanosciences, LRN-EA4682, Université de Reims Champagne-Ardenne, 51100 Reims, France, [#]Laboratory of Nano-Bioengineering, National Research Nuclear University MePhI "Moscow Engineering Physics Institute", 115409 Moscow, Russian Federation, [▽]CRCM, INSERM U1068, 13009 Marseille, France, and [⊗]Max-Planck Institute for Experimental Medicine, 37075 Goettingen, Germany

ABSTRACT Despite the widespread availability of immunohistochemical and other methodologies for screening and early detection of lung and breast cancer biomarkers, diagnosis of the early stage of cancers can be difficult and prone to error. The identification and validation of early biomarkers specific to lung and breast cancers, which would permit the development of more sensitive methods for detection of early disease onset, is urgently needed. In this paper, ultra-small and bright nanoprobes based on quantum dots (QDs) conjugated to single domain anti-HER2 (human epidermal growth factor receptor 2) antibodies (sdAbs) were applied for immunolabeling of breast and lung cancer cell lines, and their performance was compared to that of anti-HER2 monoclonal antibodies conjugated to conventional organic dyes Alexa Fluor 488 and Alexa Fluor 568. The sdAbs–QD conjugates achieved superior staining in a panel of lung cancer cell lines with differential HER2 expression. This shows their outstanding potential for the development of more sensitive assays for early detection of cancer biomarkers.

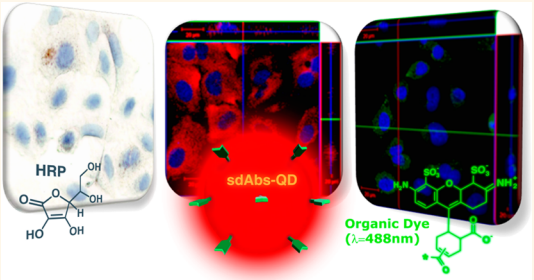

KEYWORDS: quantum dot · single domain antibodies · cancer biomarker · HER2 protein · breast cancer · lung cancer · primary macrophages · cell line co-culture · Western blot · ELISA · fluorescence lifetime imaging microscopy · optical and fluorescence properties · immunohistochemistry · confocal microscopy imaging · flow cytometry

In cancer patients, the early detection of specific cancer biomarkers can aid in the diagnosis and early treatment of these malignancies and result in a higher chance of survival. For this reason, an increased demand exists for improved cancer biomarker detection, with higher specificity and sensitivity and with fewer pitfalls than those found intrinsically in organic fluorophores or fluorescent proteins. In recent years there has been enhanced focus in the development of new probes that could be applied in the areas of molecular biology, detection, imaging and medicinal diagnostics.

Highly fluorescent semiconductor nanocrystals, quantum dots (QDs), with their unique size-dependent physical and chemical properties have been suggested as ideal candidates for this purpose.[1−8] The immense number of immunolabeling studies already published demonstrates that QDs are on their way of becoming the preferred fluorescent imaging probes.[1,9−15] Their properties, such as broad tunable fluorescence emission spectra that range from ultraviolet (UV) to infrared (IR), high surface to volume ratios and large absorption coefficients across the whole optical spectrum, make them ideal candidates for biomedical imaging, and immunofluorescent staining, especially of fixed cells and tissues.[16] For cancer biomarker detection,

* Address correspondence to rakovit@tcd.ie.

Received for review January 13, 2014 and accepted May 29, 2014.

Published online May 29, 2014
10.1021/nn500212h

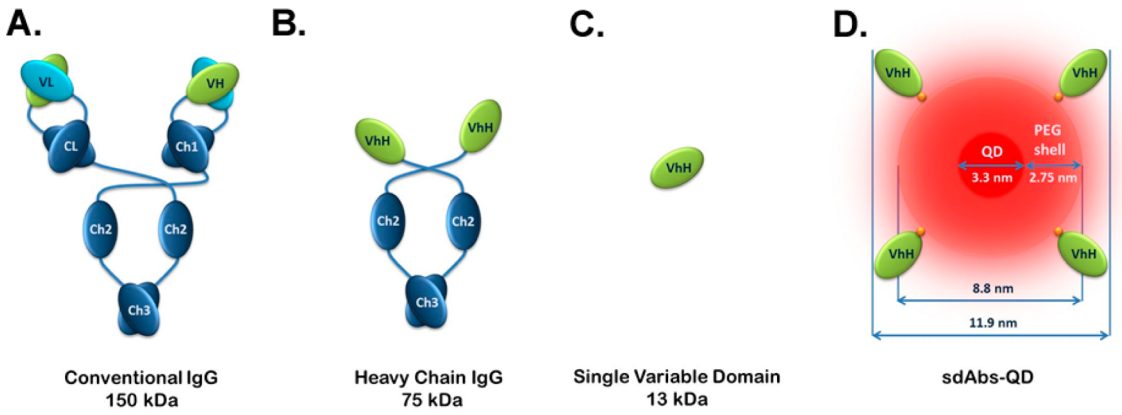

Figure 1. Structural representation of antibodies and sdAbs−QD conjugates. Conventional IgG antibody (A), heavy chain antibody (HcAb) (B), single domain antibody (sdAb or VhH) and sdAbs−QD conjugate (D). Reprinted with permission from ref 10. Copyright 2012 Elsevier.

QDs should be surface functionalized with specific recognition molecules for target detection,[17−22] such as primary or secondary antibody (Ab),[19,22,23] streptavidin,[19,22] peptides,[22,24] proteins,[22,25,26] and oligonucleotides.[22,27,28] Two most common strategies for QDs' surface functionalization with Ab involve either direct cross-linking reaction of carboxylic/amino surface groups of QDs with amino/sulfhydryl groups of Abs or an indirect interaction of streptavidin coated QDs with biotinylated Abs.[13,29] However, both approaches have their own shortcomings. Inherently, QD surface functionalization with conventional Abs (Figure 1A), also known as immunoglobulin G (IgG) molecules (molecular weight of around 150 kDa), results in the formation of large conjugates, which are not optimum if intracellular target detection is required and the process of bioconjugation can lead to denaturation of these IgG molecules rendering them inactive.[19] Additionally, the direct cross-linking strategy can result in a random Ab orientation relative to QD surface, thus obstructing active sites of Ab and impeding their activity.[30,31] The indirect approach on the other hand can result in the formation of complexes with even bigger hydrodynamic diameters and since antibodies can have several biotinylated sites, multivalent binding can occur.[31]

To solve these shortcomings, studies have been carried out with the use of antibody fragments derived from llama heavy chain antibodies conjugated to QD, which are structurally different from conventional antibodies (Figure 1B).[10,32,33] Among the main differences are the absence of two light chains in hcAbs, the heavy chains are devoid of one of their constant domains and have a modified variable domain, both of which are required for binding of light chains.[34,35] The single monomeric variable Ab domain is most often referred to as single domain antibody (sdAb) (Figure 1C), as its variable regions are composed of single protein domains, which are able to bind specifically to an antigen.[10,36,37] Despite their small molecular weight of 13 kDa, these sdAbs have comparable binding affinities to those found in conventional IgGs.[38−40]

Recently, Sukhanova and co-workers published a new method for generation of ultrasmall nanoprobes using highly oriented conjugation of sdAbs specific against carcinoembryonic antigen (CEA) and QDs and demonstrated their application to several diagnostic techniques such as flow cytometry and immunohistochemistry.[10,33] The study presented here focuses on the detection of a well-known cancer biomarker, the tyrosine kinase HER2, using QD conjugated to a sdAb directed against this biomarker (Figure 1D). HER2 receptor is found to be overexpressed in 15−30% of invasive breast cancers, but can also be found in lung, ovarian, stomach and uterine cancers.[41] The expression level of this protein in breast cancer patients is most commonly used to select patients eligible for biological cancer treatment with trastuzumab (international nonproprietary name, trade name: Herceptin), a monoclonal Ab that recognizes and blocks the HER2 protein.[42] However, the FDA (The United States Food and Drug Administration) recently approved several new HER2 targeted therapies. Lapatinib, a small molecule tyrosine kinase inhibitor, was approved for the dual targeting of HER2 and EGFR (Epidermal Growth Factor Receptor). Combination therapy consisting of the HER2 receptor antagonists Pertuzumab, trastuzumab, and the chemotherapeutic agent Docataxel was approved for the neoadjuvant treatment of patients with early stage, inflammatory or locally advanced breast cancer. Additionally, a combination of Trastuzumab and emtansine has been approved for the treatment of patients who were previously treated for metastatic breast cancer or developed tumor recurrence within six months of trastuzumab−taxane adjuvant therapy.[43,44] However, in order to accurately select patients that are eligible for this cancer treatment, it is crucial that the tests and procedures used for this purpose are both accurate and reliable.[45] HER2 protein is most often

found to be overexpressed in aggressive types of breast cancer, with its overexpression being linked to poor clinical outcome.[46,47] Since HER2 is a cell surface receptor, it is a well-known target for imaging, diagnostics and treatment.[41,42,46−48] In cancer patients, solid tumors consist of cancer cells together with many other nonmalignant cell types such as fibroblasts, endothelial cells, neutrophils, mast cells, lymphocytes and macrophages. Macrophages, in this instance, are most often referred to as tumor-associated macrophages and are key players in the process of leukocyte infiltration and cancer progression. A majority of these macrophages are found to proliferate from peripheral blood monocytes, which are recruited into the tumor mass.[49] For this reason in the present study, two different *in vitro* cell culture models were used: single cancer cell type model and co-culture model comprising of cancer cell lines with primary macrophages extracted from blood.

Here, we report on the clinically relevant diagnostic application of HER2 specific sdAbs−QD conjugates, with the use of a comparative systematic approach for the application of nanoprobes, for *in vitro* targeting and imaging of HER2 protein in breast cancer cell lines, lung cancer cell lines, and also in co-culture of the cancer cells with primary macrophages.

RESULTS AND DISCUSSION

Comparative Analysis of HER2 Expression in Breast and Lung Cancer Cell Lines. Lung and breast cancers are the most frequently diagnosed epithelial malignancies worldwide. The key determining factor in the survival rate of cancer patients is the stage at which the disease is detected and has spurred the development of more sensitive methodologies for early cancer diagnosis, which should result in higher survival rates and avoid the need for continuous monitoring of cancer progression.

One of the most common biological therapies for this malignancy is the targeting of HER2 receptor, a member of ErbB receptor tyrosine kinases family, members of which have been implicated in cellular proliferation, apoptosis, differentiation, angiogenesis, motility and invasion.[50−53] The overexpression of HER2 protein itself is associated with tumor aggressiveness and poor prognosis; however, only 25−30% of breast cancer cases are HER2 positive.[54,55] Therefore, development of accurate and sensitive method for HER2 protein detection is of extreme importance.

In this study, several lung and breast cancer cell lines were selected as models for positive/high and negative/low HER2 protein expression grades (see Table S1 in Supporting Information).

All of the lung cancer cell lines chosen were from human non-small cell lung carcinoma (NSCLC), an epithelial lung cancer that is quite insensitive to chemotherapy when compared to small cell carcinoma and is the most common type of lung cancer, accounting to 80% of all lung cancers (see Supporting Information for more details).[56]

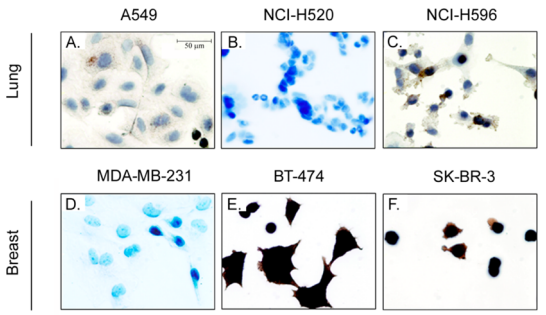

Figure 2. Immunohistochemical staining of HER2 biomarker in lung and breast cancer cell lines. Staining was scored according to the HercepTest scoring system. A549 (A) lung cancer cell line exhibited faint HER2 staining (score value = 1+), while NCI-H520 (B) lung cancer cell line demonstrated no staining (score value = 0), and NCI-H596 had similar HER2 staining to the A549 cell line. MDA-MB-231 (D) breast cancer cell line showed no staining (score value = 0); BT-474 (E) and SK-BR-3 (F) breast cancer cell lines showed strong HER2 staining (score value = 3+). Images were taken with 40× objective.

All breast cancer cell models chosen for this study were extracted from mammary gland/breast and were of invasive ductal carcinoma (IDC) origin, a type of breast cancer that accounts for 80% of diagnosed breast cancer cases. IDC initiates in the breast ducts and if left untreated can invade the surrounding breast tissue and, metastasise (see Supporting Information for more details).[57]

In this study, a number of clinically relevant methodologies were adopted in order to validate the status of HER2 expression in all lung and breast cancer cell lines used. Panels of commercially available and clinically relevant Abs were assessed for affinity to HER2 protein and the highest affinity Abs were chosen.

Cell surface HER2 expression was assessed in all cell lines with the use of clinically accepted immunohistological HercepTest (DakoCytomation, Ely, Cambridgeshire, U.K.) that is commonly used for quantitative pathological scoring and is considered to be a gold-standard in clinical practice (Figure 2). A549 and NCI-H596 lung cancer cell models were given a score of 1+ since they exhibited weak cell surface staining, and NCI-H520 lung cancer cell model was scored as 0, as no staining was observed (Figure 2A,B,C, respectively). The BT-474 and SK-BR-3 breast cancer cell lines were scored as 3+ with strong staining intensity, while MDA-MB-231 was scored as 0 with no staining (Figure 2E,F,D, respectively). These results are in line with what was previously reported in the literature and those supplied in the DakoCytomation HercepTest.

The levels of HER2 protein expression were quantified with the use of Western blot (WB) analysis and enzyme-linked immunosorbent assay (ELISA). WB analysis demonstrated that BT-474 and SK-BR-3 breast cancer cell lines had high levels of HER2 expression

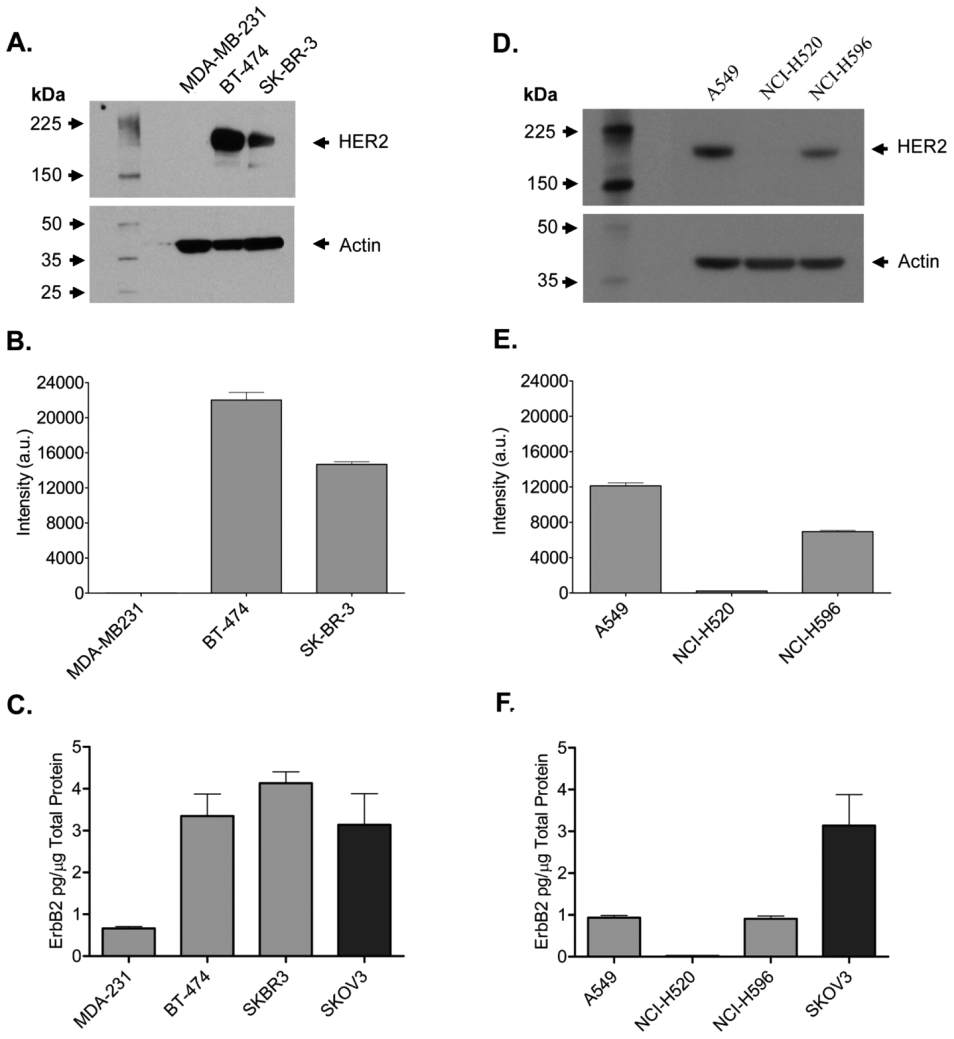

Figure 3. HER2 protein levels in breast and lung cancer cell lines. (A) Western blot analysis of HER2 protein expression levels in breast cancer cell lines. (B) Quantitative analysis of HER2 protein levels in breast cancer cell lines. (C) ELISA analysis of HER2 protein levels in whole cell lysates of breast cancer cell lines. SKOV3 lysate was used as a positive control. (D) Western blot analysis of HER2 protein levels in lung cancer cell lines. (E) Quantitative analysis of HER2 protein levels in lung cancer cell lines. (F) ELISA analysis of HER2 protein levels in whole cell lysates of lung cancer cell lines. SKOV3 lysate was used as a positive control. In Western blot analysis, HER2 levels were quantified by measuring the intensity of bands for HER2 protein and normalizing them to the actin bands on a Western blot with the use of ImageJ software. In the process of ELISA analysis, HER2 levels were quantified with the use of the human ErbB2 DuoSet ELISA Development System as per manufacturer's instructions.

and MDA-MB-231 breast cancer cell line showed no detectable HER2 protein (Figure 3A). A549 and NCI-H596 lung cancer cell lines had high levels of HER2 expression, when compared to the NCI-H520 cell line which had no detectable levels of HER2 protein (Figure 3D). Quantification of the HER2 expression levels in each of the lung and breast cancer cell line models was carried out by measuring the intensity of HER2 WB bands and standardizing them to endogenous actin protein expression levels with the use of ImageJ software (Figure 3B,E, respectively).[58] HER2 protein expression was also quantitated in whole cell lysates of lung (Figure 3E) and breast cancer cell models (Figure 3C) with the use of ELISA analysis (Figure 3E,C, respectively). Results are comparable and matched to those acquired by WB analysis. For the MDA-MB-231 cell line, low levels of HER2 expression were detected (Figure 3C), even though this was not observed by WB analysis (Figure 3A).

In all of the cell lines used, HER2 expression levels determined by HercepTest, WB and ELISA were found to be comparable to those found in literature.[59−61]

Quality Performance Assessment of sdAbs−QD and mAbs−AF Conjugates. In this study, clinically relevant, ultra-small and bright sdAbs−QD conjugates were applied for HER2 protein detection. In contrast to the traditional nanolabels consisting of the nanoparticle and the recognition molecules linked to their surface randomly, developed by us highly oriented sdAbs−QD conjugates were engineered with all sdAb antigen-recognizing sites facing outward. In such conjugates an accessibility of antigen-recognizing sites to their

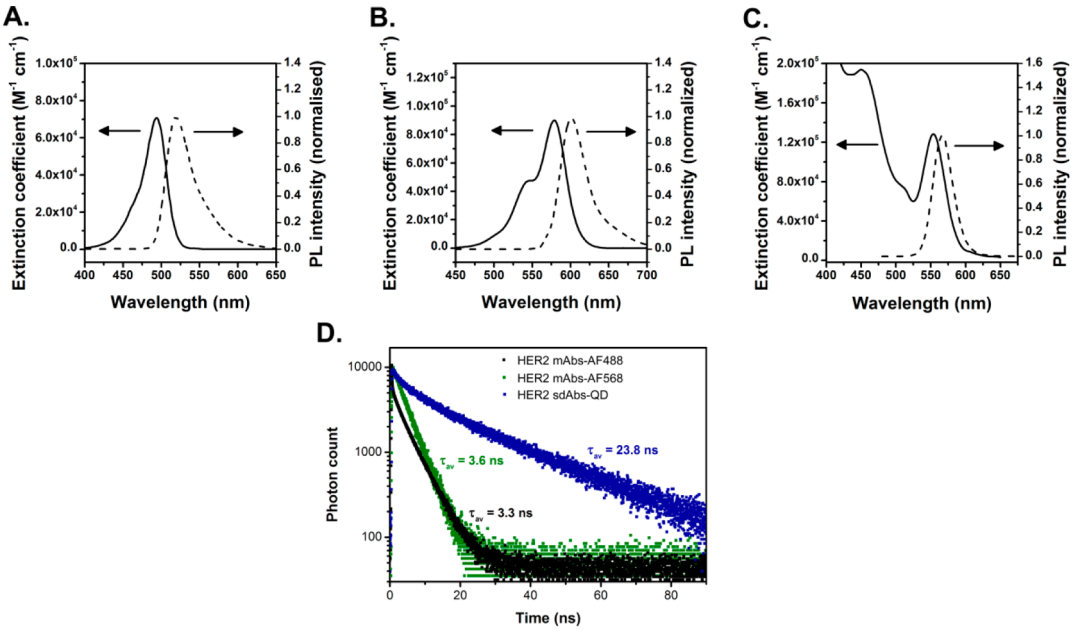

Figure 4. Absorption and normalized room temperature photoluminescence (PL) spectra for HER2 specific mAbs−AF488, mAbs−AF568, and sdAbs−QD conjugates. (A) Absorption (solid line) and PL (dashed line) spectra for mAbs−AF488 conjugates. (B) Absorption (solid line) and PL (dashed line) spectra for mAbs−AF568 conjugates. (C) Absorption (solid line) and PL (dashed line) spectra for sdAbs−QD conjugates. (D) Time-resolved fluorescence decay of solutions containing 570 nm sdAbs−QD (300 μg/mL), mAbs−AF488, and mAbs−AF568 conjugates. Data was fitted to biexponential expression to extract lifetime values.

antigens was considerably improved thus increasing the nanoprobe sensitivity.[10,33] These nanoprobes were subjected to experimental scrutiny in an attempt to imitate the strict requirements pertinent to clinically approved probes. Systematic qualitative performance assessment in terms of optical and fluorescent properties of sdAbs−QD conjugates was carried out in order to develop a highly sensitive detection assay with all of the required controls.

To compare the performance of HER2 specific sdAbs−QD conjugates two different monoclonal antibody (mAb)-Alexa Fluor (AF) conjugates were also used; mAbs−AF488 and mAbs−AF568. Quality performance characteristics of conjugates were assessed in order to set up an accurate detection. Characteristics such as optical properties were examined in order to determine the correct excitation/emission wavelengths and detection filters and to completely assess and validate the conjugates used in a clinically relevant qualitative manner. Details of these measurements can be found in the Supporting Information

The sdAbs−QD conjugates possessed a very broad absorption band (solid line in Figure 4C), extending from the exciton absorption peak at 553 nm all the way to the UV spectral region. On the other hand, mAbs−AF488 and mAbs−AF568 samples both absorbed over narrow ranges of ∼130 nm. This comparison demonstrates a possible advantage of QDs in multiplexing applications. The broad absorption of QDs from visible to deep UV allows for simultaneous excitation of multiple samples with the same light source. In contrast, when using fluorescent dyes for multiplexing experiments several light sources are required, each matched to the absorption spectrum of the dye. Fluorescence spectra of mAbs−AF488, mAbs−AF568, and sdAbs−QD were centered at 520, 600, and 567 nm, respectively (Figure 4A−C). To achieve confocal microscopy contrast definition, the mAbs−AF488 and sdAbs−QD conjugates were excited at 488 nm and the long-pass (LP) 530 nm filter and bandpass (BP) 530−600 nm filter were used for the detection of fluorescence, respectively. The mAbs−AF568 conjugates were excited at 561 nm and the signal was detected with the use of the LP575 filter.

Another advantage of using QDs for imaging applications is that their extinction coefficients tend to be higher than those of standard dyes. For example, using a protocol described by Yu *et al.*,[62] the extinction coefficient of sdAbs−QD conjugates was determined to be ∼130 kM^{-1} cm^{-1} at 554 nm (optimum excitation), while the extinction coefficients of mAbs−AF488 and mAbs−AF568 at their absorption maxima were 71 and 90 kM^{-1} cm^{-1}, respectively. At 488 nm (excitation wavelength used for confocal imaging), QDs' extinction coefficient of ∼100 kM^{-1} cm^{-1} was significantly higher than that of ∼65 kM^{-1} cm^{-1} of the green emitting mAbs−AF488, despite suboptimal excitation of the QD sample. These considerations allow for the conclusion that QDs and dyes used in our experiments have comparable brightness, despite significantly higher emission quantum yields of the AF dyes 92% and 70% *versus* QDs (∼40%).

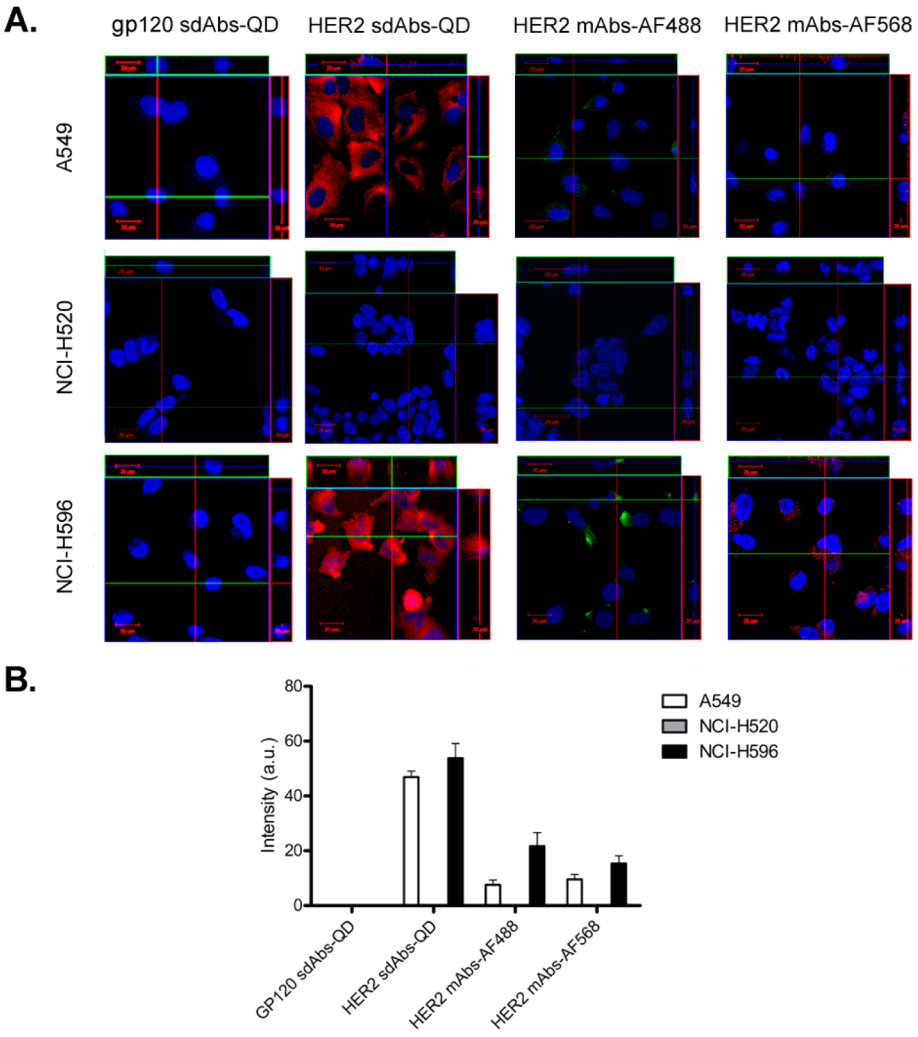

Figure 5. HER2 protein expression in positive (A549 and NCI-H596) and negative (NCI-H520) lung cancer cell models analyzed with confocal microscopy. (A) Cells were labeled with HER2 specific mAbs−AF488, mAbs−AF568, sdAbs−QD, and gp120 specific sdAbs−QD conjugates. gp120 specific sdAbs−QD conjugates were used as a control for nonspecific QD binding. (B) HER2 protein staining intensity quantification in lung and breast cancer cell models was analyzed with confocal microscopy with the use of ImageJ software. HER2 protein staining intensity quantification in lung and breast cancer cell models analyzed with confocal microscopy.

In addition to the spectral comparison, the fluorescence decay properties of the HER2 specific mAbs−AF488, mAbs−AF568, and the sdAbs−QD conjugates were examined (Figure 4D). Details of these measurements can be found in the Methods section. Overall, the lifetime values obtained for all of the samples are typical when compared to literature values in closely matching, reproduced conditions. The lifetime of the mAbs−AF488 conjugates was found to be 3.3 ns and the lifetime of mAbs−AF568 conjugates was found to be approximately 3.6 ns (Figure 4D), which is similar to the lifetime of the autofluorescence of the cellular components, such as bound NADH (nicotinamide adenine dinucleotide) which has lifetime of approximately 2 ns.[63] The lifetime of sdAbs−QD conjugates' fluorescence (23.8 ns) was significantly larger than that of the mAb−AF488 and mAb−AF568, and was consistent with those published in literature for protein−QD conjugates.[64,65] Importantly, and in contrast to AF dyes, QDs' lifetime value was an order of magnitude higher than the lifetime of autofluorescence of cellular components. This indicates that in FLIM (Fluorescence-Lifetime Imaging Microscopy) imaging of biological samples higher contrast can be achieved with sdAbs−QD conjugates than with mAbs−AF488 and mAbs, resulting in improved sensitivity of the imaging technique.

Comparison of QD-Based Probes Performance with Conventional Dyes. The performance of sdAbs−QD conjugates was examined in chosen lung and breast cancer cell models with the use of confocal microscopy and flow cytometry. sdAbs−QD conjugates specific for envelope glycoprotein gp120 exposed on the surface of the HIV (Human Immunodeficiency Virus) envelope were used as the control samples for nonspecific staining of QDs.[36] This control was chosen as these

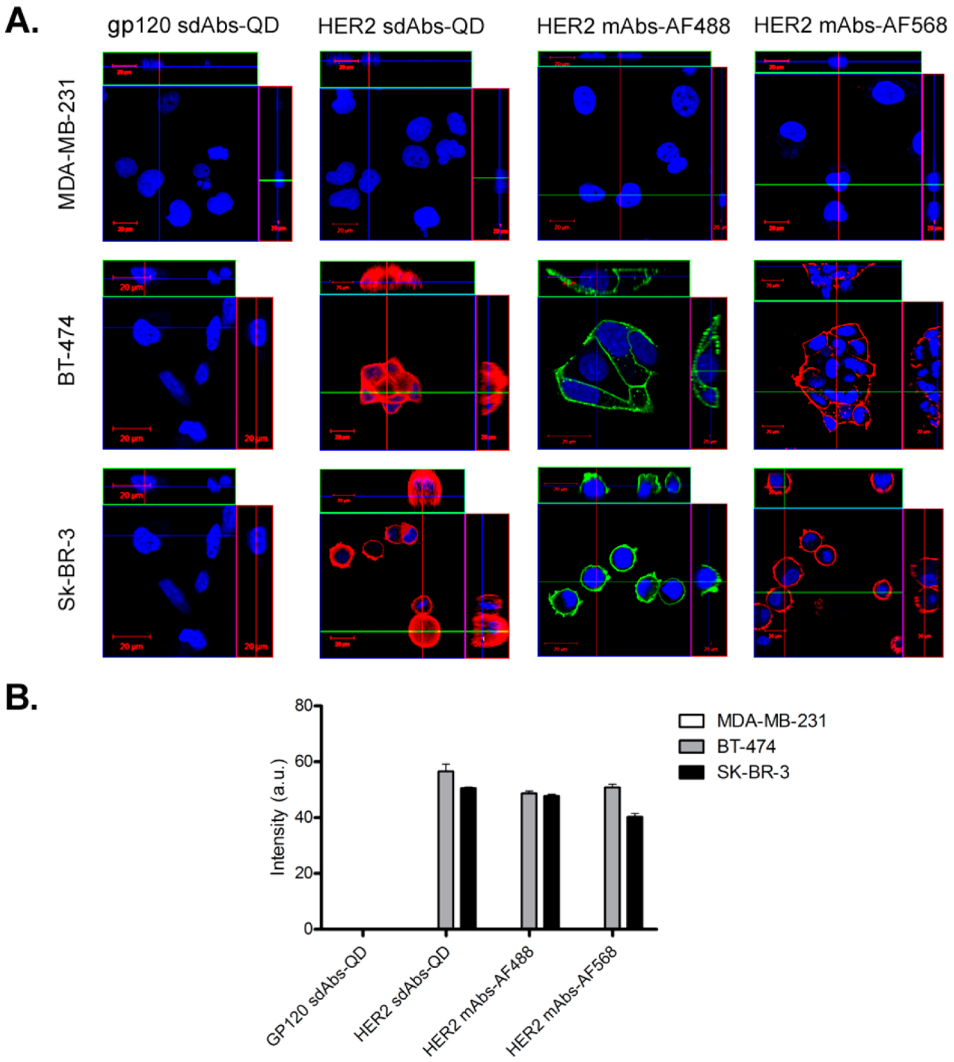

Figure 6. HER2 protein expression in positive (BT-474 and SK-BR-3) and negative (MDA-MB-231) breast cancer cell models analyzed with confocal microscopy. (A) Cells were labeled with HER2 specific mAbs−AF488, mAbs−AF568, sdAbs−QD, and gp120 specific sdAbs−QD conjugates. gp120 specific sdAbs−QD conjugates were used as a control for nonspecific QD binding. (B) HER2 protein staining intensity quantification in lung and breast cancer cell models was analyzed with confocal microscopy with the use of ImageJ software. HER2 protein staining intensity quantification in lung and breast cancer cell models was analyzed with confocal microscopy.

QDs should only detect gp120 protein and as no staining should be observed in breast and lung cancer cell lines.

Confocal microscopy analysis of HER2 protein was carried out in lung (Figure 5) and breast cancer cell models (Figure 6) and in co-culture with primary macrophages (Figures 7 and 8). A brighter and higher level of intensity of HER2 labeling in low expressing lung cancer cell lines (A549 and NCI-H596) was achieved with the use of sdAbs−QD when compared to mAbs−AF488 and mAbs−AF568 conjugates' (Figure 5) staining, which was found to be very weak. Confocal microscopy analysis of high HER2 expressing breast cancer cell lines (BT-474 and SK-BR-3) demonstrated good staining with all three conjugates used, providing images of good quality with comparable high intensity signal (Figure 6). HER2 negative lung and breast cancer cell lines, NCI-H520 and MDA-MB-231, respectively, showed no HER2 labeling, which was also the case when cells were incubated with gp120 specific sdAbs−QD conjugates.

Tumor cells are rarely presented as an isolated population and commonly co-exist with other cell types; therefore, in this work we have used human primary macrophages (PM) in a co-culture with selected lung and breast cancer cell lines (Table S1). To be able to distinguish PM cells from cancer cells, they were labeled with CD11a (Integrin, alpha L) specific mAbs-APC (Allophycocyanin), a transmembrane glycoprotein that is expressed on lymphocytes, monocytes, macrophages, neutrophils, basophils and eosinophils making it a good control for specific staining of primary macrophages. Lung (Figure 7A) and breast (Figure 8A) cancer cell lines were specifically labeled with either HER2 specific sdAbs−QD or mAbs−AF488 conjugates. Staining efficiencies of sdAbs−QD and mAbs−AF488

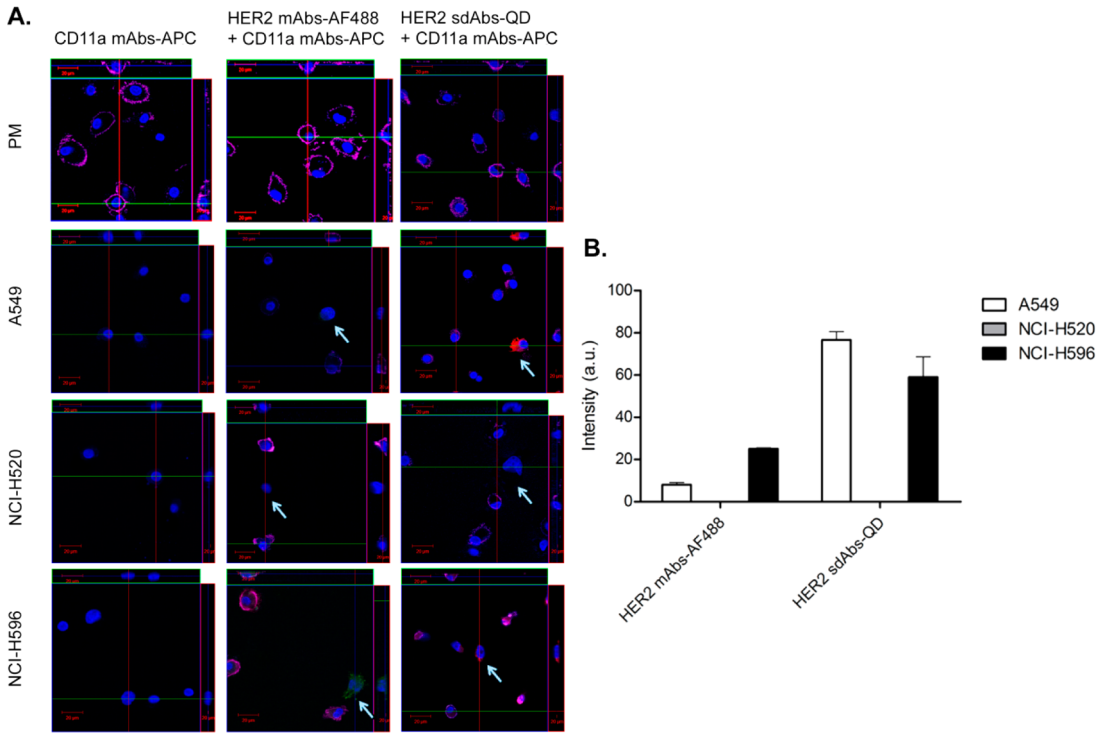

Figure 7. Single lung cancer cell (A549, NCI-H520 and NCI-H596) detection in co-culture with primary macrophages. (A) Lung cancer cell lines were labeled with HER2 specific mAbs–AF488 and sdAbs–QD conjugates (white arrows) and primary macrophage cells were labeled with CD11a specific mAbs–APC conjugates. (B) HER2 protein staining intensity quantification in single lung models in co-culture experiment with primary macrophages was analyzed with confocal microscopy.

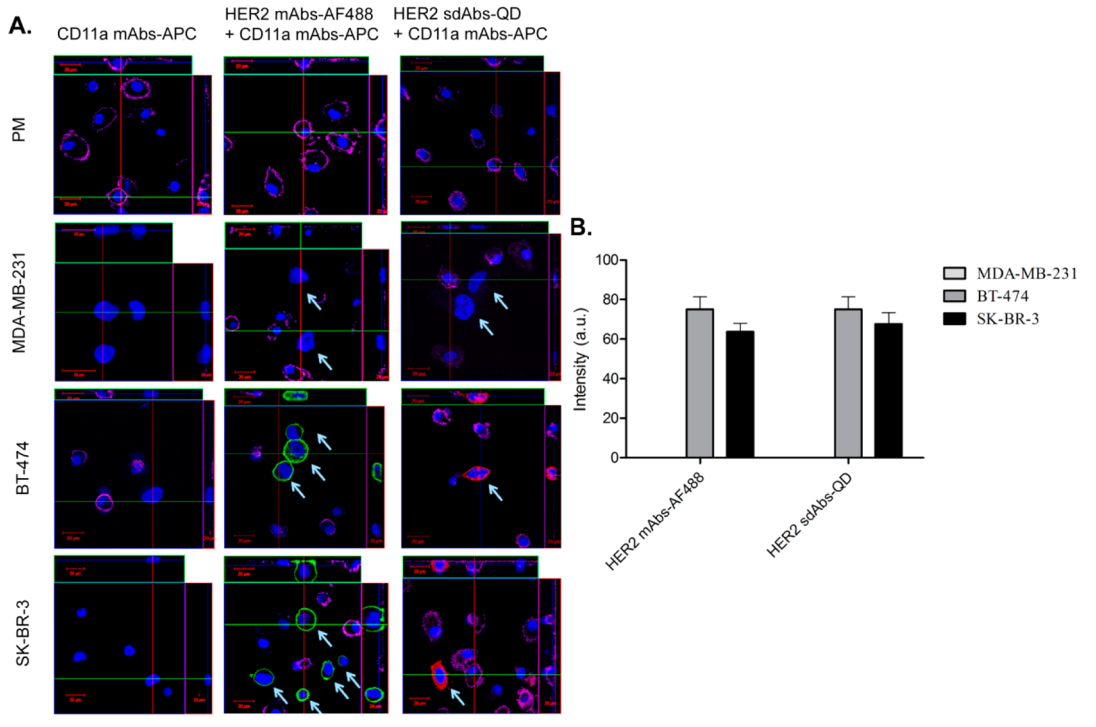

Figure 8. Single breast cancer cell (MDA-MB-231, SK-BR-3 and BT-474) detection in co-culture with primary macrophages. (A) Breast cancer cell lines were labeled with HER2 specific mAbs–AF488 and sdAbs–QD conjugates (white arrows) and primary macrophage cells were labeled with CD11a specific mAbs–APC conjugates. (B) HER2 protein staining intensity quantification in single breast models in co-culture experiment with primary macrophages was analyzed with confocal microscopy.

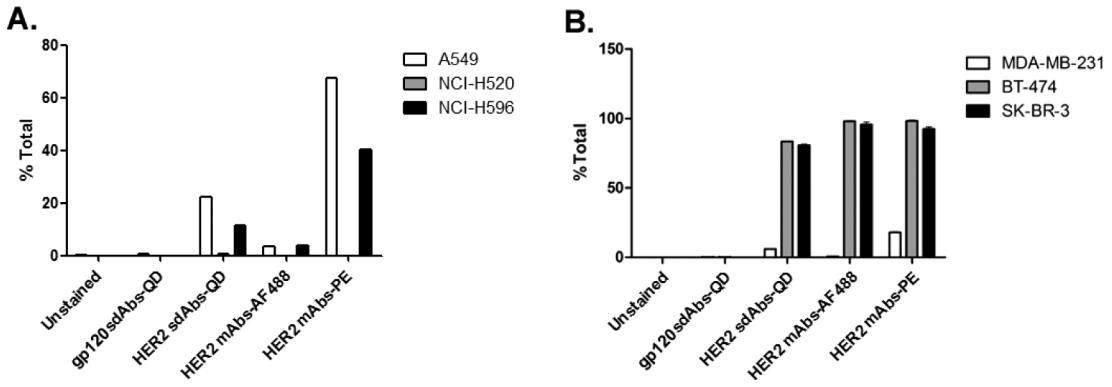

Figure 9. Flow cytometry analysis of HER2 protein expression in lung (A) and breast (B) cancer cell models. Cells were labeled with HER2 specific mAbs−AF488, mAbs−PE, and sdAbs−QD conjugates. gp120 specific sdAbs−QD conjugates were used as control for nonspecific QD binding (10 000 events per run, n = 3). Representative flow cytometry histograms for HER2 detection in lung and breast cancer cell models can be found in Figures S3 and S4, respectively.

conjugates for single cancer cell detection were compared with the use of confocal microscopy analysis and quantified with the use of ImageJ software (NIH) (Figures 7B and 8B). In lung cancer cell lines, the sdAbs−QD conjugates attained much brighter and higher level of intensity of HER2 for HER2 expression (A549 and NCI-H596) when compared to mAb−AF488 staining (Figure 7) where it was approaching undetectable levels. High HER2 expressing breast cancer cell lines (BT-474 and SK-BR-3) demonstrated good HER2 labeling with both sdAbs−QD and mAbs−AF488 conjugates provided good quality images with comparable intensity staining values (Figure 8). Both conjugates demonstrated no HER2 labeling in NCI-H520 lung cancer cell line (Figure 7) and MDA-MB-231 breast cancer cell line (Figure 8). PM cells were clearly and distinguishably visible as a discrete cell population (Figures 7A and 8A).

Consequently, sdAbs−QD conjugates were shown to have superior performance in low expressing lung cancer cell lines both on their own (Figure 5) and in co-culture with primary macrophages (Figure 7) with distinguishable labeling difference when compared to conventional organic dyes. Confocal microscopy analysis of levels of intensity of staining allowed for a more accurate quantification of HER2 expression levels when compared to the gold standard IHC HercepTest in low expressing lung cancer cell lines (Figure 2). One possible explanation could be the fact that sdAbs−QD are much smaller conjugates when compared to the size of mAbs−AF conjugates and sdAbs have previously been reported to have a potential to penetrate cavities in target antigens, such as enzyme active sites and to bind targets that are usually inaccessible when using monoclonal antibodies.[38]

Flow cytometry analysis of HER2 protein was also carried out in lung and breast cancer cell models with the use of HER2 specific mAbs−AF488, mAbs−PE (Phycoerythrin) and sdAbs−QD conjugates. Conjugate efficiency was measured on BT-474 and MDA-MB-231 cell lines as the percentage of total staining intensity (% TSI) values, obtained with increasing concentrations of mAbs−AF488, mAbs−PE and sdAbs−QD conjugates (Figure S1). The optimal concentrations for staining with mAbs−AF488, mAbs−PE, and sdAbs−QD conjugates were found to be 10, 0.2, and 30 μg/mL, respectively. For all of the subsequent flow cytometry experiments, these concentrations were used.

As we deem it essential for all new clinically relevant standard probes and as part of standard operating procedure (SOP), the potential cytotoxicity of QD conjugates was examined in all of the cancer cell models. Due to the intrinsically toxic nature of CdSe QDs, both to human health and the environment, the development of SOPs as well as proper waste disposal should be carried out in parallel with the establishment of their applications. In this study, cytotoxicity tests were performed in lung and breast cancer cell lines exposed to 30 μg/mL of sdAbs−QD conjugates over 3 h at 4 °C (Figure S2). No detectable level of cytotoxicity was observed in these assays.

Conversely to confocal microscopy, in flow cytometry analysis, traditional mAbs conjugates performed better when compared to sdAbs−QDs, even in low HER2 expressing cell lines (Figures 9, S3 and S4). An explanation for this could be that fluorescent dyes emit more photons than QDs for the length of time that they are being excited by laser light; therefore the application of QDs for flow cytometry requires further optimization.

Overall, the successful detection of HER2 protein was achieved with the use of sdAbs−QD conjugates and the efficiency of the targeting and labeling was compared to that of monoclonal antibodies conjugated to conventional dyes. With the use of confocal microscopy, it was shown that HER2 specific sdAbs−QD conjugates displayed an exceptional superiority over conventional dyes for detection of low expressing HER2 lung cancer cell lines in single or co-culture configuration with primary macrophages.

CONCLUSIONS

In this study, a superior advantage of using highly oriented sdAbs–QD conjugates specific to the HER2 cancer biomarker for the detection of low expression levels of HER2 with confocal microscopy imaging has been demonstrated. Obtained results hold a great potential for the application of these nanoprobes in the development of extremely sensitive and specific clinical assays for early cancer biomarker detection.

Mimicking the *in vivo* tumor microenvironment, co-culture experiments demonstrated that such engineered QD conjugates can potentially be used for cancer cell detection with more sensitivity and specificity than that currently found in gold standard methodologies for cancer cell detection. This could ultimately pave the way to the application of these QDs as outstanding labeling probes in the field of cancer research and diagnostics.

METHODS

Reagents and Antibodies. Dulbecco's modified Eagle medium (DMEM), RPMI (Roswell Park Memorial Institute) 1640 medium, F12 Nutrient Mixture, McCoy's 5A Medium, penicillin–streptomycin solution and Fetal Bovine Serum (FBS) were obtained from Gibco (Invitrogen, BioSciences, Ltd., Dublin, Ireland). Sodium Pyruvate was purchased from Sigma-Aldrich (Sigma-Aldrich Corporation). HER2 specific mAbs (Alexa Fluor 488 anti-human CD340 (erbB2/Her2) and purified anti-human CD340 (erbB2/HER-2) antibodies) were obtained from BioLegend. Alexa Fluor 568 Protein Labeling Kit was from (Molecular Probes, Life Technologies, Ireland). HER2 specific mAbs–PE (HER-2/neu) was purchased from BD Biosciences (Becton, Dickinson and Company, Ltd., U.K.) and anti-HER2 mAb used for Western blotting was obtained from EMD Millipore Corporation (Billerica, MA). HercepTest was obtained from Dako Diagnostics (Ireland Ltd.). All cells were purchased from ATCC (LGC Standards) (Middlesex, U.K.). All of the other reagents, unless specifically indicated, were from Sigma (St. Louis, MO).

Cell Culture and Seeding Density. Human epithelial lung cancer (A549, NCI-H520 and NCI-H596) and breast cancer cell lines (MDA-MB-231, BT-474, SK-BR-3) and human primary macrophages extracted from blood were used in this study. A549 cell line was cultured in F12 medium and MDA-MB-231 was cultured in DMEM medium supplemented with 10% FBS and 1% penicillin–streptomycin solution (10 000 units/mL). BT-474 cell line was cultured in RPMI 1640 medium supplemented with 10% FBS, sodium pyruvate (1 mM) and 1% penicillin–streptomycin solution (10 000 units/m). NCI-H520 and NCI-H596 cell lines were cultured in RPMI 1640 medium supplemented with 10% FBS and 20% FBS, respectively, and 1% penicillin–streptomycin solution (10 000 units/mL). SK-BR-3 cell line was grown in McCoy's 5A medium supplemented with 10% FBS and 1% penicillin–streptomycin solution (10 000 units/mL). For co-culture experiments, peripheral blood mononuclear cells (PBMCs) were isolated from the buffy coat of anonymous healthy donors (provided, with permission of the Irish Blood Transfusion Service) by centrifugation on Lymphoprep (Axis-Shield, Oslo, Norway) density gradient, washed and resuspended in RPMI-1640 culture medium, supplemented with 10% pooled human serum type AB (Sigma), with 100 μg of penicillin/mL and 100 mg of streptomycin/mL (Sigma, P4333). Cells were seeded at a density of 5×10^6 cells/mL onto glass coverslips in 24 well tissue-culture plates (Fisher Scientific Ireland Ltd., Dublin, Ireland). Nonadherent cells were removed by washing with warm medium every 2–3 days. Primary macrophages were cultured for 7 days before addition of cancer cells. On eighth day, appropriate cancer cell lines were added (5000 cells/well) to the primary macrophages and left to attach for approximately 3 h. Once attached, cells were fixed with the use of 3.7% paraformaldehyde. For confocal and immunohistochemistry studies, cells were seeded in sterile Millicell EZ 8-well glass slides (Merck Millipore) at 15 000 cells per well that were maintained at 37 °C and 5% CO_2. Cells were then fixed with 3.7% paraformaldehyde as described.[66] For flow cytometry experiment, cell lines were cultured in T75 flasks until 80% confluency and were maintained at 37 °C and 5% CO_2 until analysis. At the time of analysis, cells were dissociated with 0.5 mM EDTA solution and were washed twice with 0.5% bovine serum albumin solution made up in PBS.

Whole Cell Protein Extraction. All steps of the whole cell protein extraction were carried out on ice. Lung and breast cancer cells were washed once with sterile PBS and scraped into 1 mL of PBS solution. Cells were then centrifuged at 2000*g* for 5 min at 4 °C, and the cell pellet was resuspended in 50 μL of lysis buffer (20 mM HEPES (pH 7.6), 400 mM NaCl, 1 mM EDTA (pH 8.0), 5 mM NaF, 40 mM Na_3VO_4, 25% glycerol, 0.1% NP40 (IGEPAL 630), 1 mM PMSF, 1 mM DTT, protease inhibitors) and incubated on ice for 10 min. Cells were passed through a 25 G needle (Neolus, Terumo, Europe NV, Leuven, Belgium) 10 times and allowed to incubate on ice for further 40 min. Samples were centrifuged for 10 min at 17 200*g* at 4 °C and the supernatant containing total protein extract was removed, total protein content was determined, and samples were stored at −80 °C until further analysis.

Total Protein Quantification. Extracted lung and breast protein samples were defrosted on ice. Total protein content in each sample was measured by the Bradford assay through comparison to a standard curve generated from colorimetric measurement (Coomassie blue) of serially diluted albumin standard (#23209, Thermo Scientific, Rockford, IL) at 495 nm with the use of UV–vis spectrophotometer (Epoch, BioTek, U.K.).

Quantum Dots and Alexa Fluor 568 mAb Conjugates. Cd/ZnS core/shell QDs emitting fluorescence at 570 nm were conjugated to HER2 or gp120 specific sdAbs through cysteine residue specifically integrated into the sdAbs C-terminus. The details of the synthesis and stabilization of QDs in aqueous buffers and biological fluids can be found elsewhere.[10]

The procedure of the oriented conjugation of the HER2-specific sdAbs with the QDs was adapted from the protocol described in Sukhanova *et al.*.[33] HER2 specific mAbs–AF568 conjugate was prepared according to the manufacturer's instructions with the use of Alexa Fluor 568 Protein Labeling Kit.

Western Blot Analysis. HER2 expression levels in breast and lung cancer cell lines were detected by carrying out denaturing, nonreducing SDS-PAGE electrophoresis. Proteins were separated on NuPAGE Bis-Tris SDS-PAGE (4–12%) precast mini-gels with the use of XCell *SureLock* Mini-Cell (Invitrogen Ltd., U.K.) and discontinuous NuPAGE MOPS buffering system (Invitrogen Ltd., U.K.). All samples were made up by mixing an appropriate volume with 4× NuPAGE LDS sample buffer (Invitrogen Ltd., U.K.) and heating samples at 98 °C for 2 min. Bis-Tris gels were loaded with 60 μg protein per sample lane and electrophoresed at constant 200 V for approximately 1 h. Proteins were then electroblotted onto polyvinylidene fluoride (PVDF) Immobilion P membrane (EMD Millipore Corporation, Billerica, MA) at 30 V for 2 h with the use of XCell II Blot Module (Invitrogen Ltd., U.K.). Equal loading amounts were verified by staining membrane with Ponceau S (Sigma-Aldrich Corporation,) stain. SNAP i.d. Protein Detection System (EMD Millipore Corporation, Billerica, MA) was used to process membranes according to the manufacturer's instructions. Briefly, blocking buffer consisting of 0.5% nonfat dried milk powder (Marvel, U.K.) in TBST (20 mM Tris-HCl, 150 mM NaCl and 0.1% Tween-20) was added to the SNAP i.d. (EMD Millipore Corporation, Billerica, MA) holders containing transferred blots and vacuum was immediately applied. Primary anti-HER2 mAb (EMD Millipore Corporation, Billerica, MA), diluted 1:300 in blocking buffer, was added and membranes were

left to incubate for 10 min at room temperature. Vacuum was applied and membranes were washed three times with TBST buffer. HRP-conjugated secondary Ab, diluted 1:3000 in blocking buffer, was added and blots were incubated for further 10 min at room temperature. Vacuum was applied again and the membranes were washed three times with TBST buffer. HER2 protein bands were detected with the using Luminata Western HRP Substrate (EMD Millipore Corporation, Billerica, MA) enhanced chemiluminescent detection system and subsequent exposure to Kodak light-sensitive film.

ELISA. HER2 protein levels were measured in the whole cell lysate of breast and lung cell lines using the human ErbB2 DuoSet ELISA Development System (#DY1129, R&D Systems), and normalized to total protein concentration. Quantification of HER2 concentration in each sample was carried out using the human ErbB2 DuoSet ELISA Development System as per manufacturer's instructions. HER2 concentration in each sample was determined through comparison to a standard curve generated from colorimetric measurement (Tetramethylbenzidine, Calbiochem, EMD Millipore Corporation, Billerica, MA) of serially diluted, purified recombinant ErbB2 (supplied) at 450 nm (Epoch, BioTek, U.K.). Final HER2 concentration was expressed as a fraction of total protein content per sample and values were presented as mean ± SEM (GraphPad Prism5, GraphPad Software, Inc.).

Immunohistochemistry. In this study, HER2 protein expression was histologically evaluated in breast and lung cancer cell lines using HercepTest (Dako Diagnostics Ireland Ltd.) according to the manufacturer's instructions supplied in the kit. Breast and lung cancer cell lines grown on Millicell EZ 8-well glass slides were immersed in preheated Dako Epitope Retrieval Solution (0.1 mol/L citrate buffer with a detergent), incubated for 40 min at 95−99 °C, and then left to cool-down for 20 min at room temperature. Peroxidase-Blocking Reagent (3% hydrogen peroxide containing 15 mmol/L sodium azide) was added for 5 min and samples were incubated for a further 30 min with rabbit anti-human HER2 protein or negative control reagent (immunoglobulin fraction of normal rabbit serum), supplied prediluted in the HercepTest kit. Ab was detected by the exposure of sample slides to visualization reagent (dextran polymer conjugated with horseradish peroxidase and affinity-isolated goat anti-rabbit immunoglobulins) for 30 min, incubation with substrate chromogen solution (DAB) for 10 min and counterstaining with hematoxylin. Positive control slides, supplied in HercepTest kit, were used in each experiment containing sections of three formalin-fixed paraffin-embedded breast carcinoma cell lines representing different levels of HER2 protein expression: MDA-231 (0), MDA 175 (1+), and SK-BR-3 (3+). For quantitation of HER2 expression in the tested cell lines, HercepTest kit scoring guidelines were used, with scores of 0 or 1+ being considered negative for HER2 overexpression, 2+ being weak positive, and 3+ indicating strong positivity. For the purposes of this study, two negative cell lines, two cell lines with cell surface expression score of 1+, and two cell lines with a score of 3+ were used. This variety of HER2 expression levels provided ideal test cell models for the application of HER2 specific sdAbs−QD, mAbs−AF488 and mAbs−AF568 conjugates as fluorescent probes and the comparison of both.

Time-Resolved Photoluminescence Decays Measurement. Time-resolved photoluminescence (PL) decays of HER2 specific mAbs−AF488, mAbs−AF568 and sdAbs−QD conjugates were measured using time-correlated single photon counting on a MicroTime200 setup (PicoQuant, Berlin). Measurements were performed in ambient conditions at room temperature. All of the labeling probes were diluted to a concentration of 0.3 mg/mL. Samples were excited by 480 nm picosecond laser pulses (PicoQuant LDH-480 laser head controlled by PDL-800B driver), focused by a 100× oil-immersion objective. Emitted light was collected by the same objective and passed through a 50 μm pinhole before detection. The overall temporal resolution of the setup was ∼150 ps. The measured PL decays were fitted using nonlinear squares analysis (SymPhoTime, PicoQuant) to an equation of the form

$$I(t) \propto \sum_i \alpha_i \exp(-t/\tau_i) \quad (1)$$

where τ_i are the PL decay lifetimes and α_i are the corresponding pre-exponential factors, taking into account the normalization of the initial point in the decay to unity. Weighted residuals and χ^2 values were used to judge the quality of the fit. A fit with χ^2 value between 1.0 and 1.1 was considered to be good. The τ_i and α_i values obtained from the fit were then used to calculate the average lifetime τ_{av} using

$$\tau_{\mathrm{av}} = \frac{\sum \alpha_i \tau_i^2}{\sum \alpha_i \tau_i} \quad (2)$$

Confocal Microscopy. The HER2 positive and negative lung and breast cancer cell lines were fixed with 3.7% (w/v) paraformaldehyde in phosphate-buffered saline and blocked with 10% BSA solution made up in PBS for 30 min at room temperature. HER2 specific mAbs−AF488 and mAbs−AF568 (1:50 dilution) conjugates, HER2 specific sdAbs−QD or gp120 specific sdAbs−QD (0.1 mg/mL) conjugates made up in 2% BSA solution and in PBS were then added; cells were incubated for 1 h in the dark at room temperature and washed three times with PBS. Cell nuclei were then stained by addition of Hoechst stain (Sigma-Aldrich Corporation), diluted 1:500 in 2% BSA solution made up in PBS for 30 min at room temperature, followed by three washes with PBS. Slides were mounted with Dako Fluorescent Mounting Medium (Dako) for slides incubated with mAbs−AF488 and mAbs−AF568 conjugates and Qmount Qdot Mounting Media (Invitrogen, Biosciences) for slides stained with sdAbs−QD conjugates. For single lung (A549, NCI-H596 and NCI-H520) and breast (BT-474, SK-BR-3 and MDA-MB-231) cancer cell detection in co-culture experiment with primary macrophages, all slides were initially blocked with 10% BSA solution made up in PBS for 30 min at room temperature. CD11a specific mAbs-APC (1:50 dilution) made up in 2% BSA was then added to all of the slides and slides were incubated for 1 h in the dark at room temperature, slides were then washed 3 times with PBS, and HER2 specific mAbs−AF488 (1:50 dilution) or sdAbs−QD (0.1 mg/mL) conjugates were added to appropriate slides and samples were incubated for 1 h in the dark at room temperature. Cell nuclei were then stained by addition of Hoechst stain (Sigma-Aldrich Corporation), diluted 1:500 in 2% BSA solution made up in PBS for 30 min at room temperature, followed by three washes with PBS. Slides were mounted with Dako Fluorescent Mounting Medium (Dako) for slides incubated with mAbs−AF488 and mAbs-APC and Qmount Qdot Mounting Media (Invitrogen, Biosciences) for slides stained with sdAbsQD conjugates. High resolution images of HER2 protein in lung and breast cancer cell lines were taken with the Ziess LSM Meta-510 confocal microscope (Carl Zeiss, Axiovert, Germany). Two channel qualitative imaging was carried out by acquisition of Z-stack images, using the 63x oil immersion objective. For mAbs−AF488 staining and sdAbs−QD staining laser excitation of 488 nm was used with LP530 nm filter and BP530−600, respectively, for the mAbs−AF568 a laser excitation of 561 nm was used with the LP575 filter, for Hoechst 405 nm laser was used with the BP420−480 filter and for mAbs-APC an excitation of 633 nm was used with the LP650 filter.

Flow Cytometry. The HER2 status of lung and breast cancer cell lines was determined with the use of flow cytometry. Cells, grown to 80% confluency in T75 flasks, were detached with 0.05% EDTA in Ca^{2+} and Mg^{2+} free PBS and washed twice with FACS buffer (D-PBS with Ca^{2+}/Mg^{2+} supplemented with 0.5% bovine serum albumin (BSA)). Cells, 100 000 cells per 50 μL of FACS buffer, were incubated with HER2 specific sdAbs−QD, mAbs−AF488 and mAbs−AF568 conjugates and gp120 specific sdAbs−QD conjugates for duration of 1 h, in dark at 4 °C.

The optimal staining concentrations of HER2 specific mAbs−AF488, mAbs−PE and sdAbs−QD conjugates were determined by incubating BT-474 and MDA-MB-231 cells with ranging concentrations of mAbs−AF488 conjugates from 0 to 120 μg/mL, mAbs−PE concentrations ranging from 0 to 0.8 μg/mL or 570 nm sdAbs−QD conjugates with concentrations ranging from 0 to 120 μg/mL for a duration of 1 h, in the dark at 4 °C. Finally, HER2 protein expression levels in all lung and breast cancer cell lines were determined with the use of mAbs−AF488 (10 μg/mL), mAbs−PE (0.2 μg/mL) and sdAbs−QD (30 μg/mL) (n = 3).

gp120 specific sdAbs–QDs (30 μg/mL) were used as control for nonspecific binding.

For the cytotoxicity experiment, 200 000 cells were dissociated mechanically and washed twice with FACS buffer (D-PBS with Ca^{2+}/Mg^{2+} supplemented with 0.5% BSA). Cells were resuspended at 8×10^6 cells/mL concentration in FACS buffer supplemented with 0.2% NaN_3. Thereafter, 25 μL of each cell suspension was incubated at 4 °C with 25 μL of a dilution series of HER2 specific sdAbs–QD conjugates (concentrations ranging from 0 to 120 μg/mL, see Supporting Information Table 1). After a 50 min incubation on ice, 2.5 μL of 7-AAD (BD Biosciences) was added. After further 10 min incubation on ice, cells were washed once with FACS buffer and analyzed subsequently on a FACS Canto II device. Staining was detected and cell doublets were excluded during analysis. The percentage of death was then calculated by quantifying 7-AAD positive cells and normalizing to the total 7-AAD negative cells.

Flow cytometry cytotoxicity experiment was performed using a BD FACSCanto II (BD, Becton, Dickinson) device and the rest of flow cytometry results were obtained with the use of BD FACSCanto system (BD, Becton, Dickinson). A 488 nm argon laser was used for excitation, and fluorescence intensity of sdAbs9–QD was measured between 564 and 606 nm. Fluorescence intensity of AF488 coupled Abs was measured between 515 and 545 nm. Data and gated analysis were performed with BD FACSDiva software.

High Content Screening and Analysis. Cells were seeded in 96-well plates (Nalge Nunc International) at a seeding density of 1.5×10^4 cells/(100 μL/well) and allowed to attach overnight. Cells were exposed to sdAbs–QDs at a concentration of 30 μg/mL and incubated for 3 h. Following incubation, cells were washed with PBS, fixed using prewarmed (37 °C) 3.7% paraformaldehyde, washed again with PBS, and stained for 10 min with Hoeschst 33342 (Sigma-Aldrich Corporation) to visualize the nuclei. Cytotoxicity testing was performed using the IN Cell Analyzer 1000 microscope (GE Healthcare, U.K.). All cells were visualized by scanning the full well surface area and the acquired images were automatically analyzed by the IN Cell Investigator software (version 1.6) (GE Healthcare, U.K.). The total cell count, normalized to the negative control, was monitored post incubation with sdAbs–QDs.

Conflict of Interest: The authors declare no competing financial interest.

Acknowledgment. The authors would like to thank Prof. Yury Rakovich (University of the Basque Country (UPV/EHU), Donostia International Physics Center (DIPC), Spain), Dr. Fernanda Ramos (Max-Planck-Institut für Experimentelle Medizin, Germany), Dr. Jennifer Conroy and Laura Kickham (Trinity College Dublin, Ireland) who provided valuable assistance to the undertaking of the research summarized in this manuscript. This work was partially funded by EC FP7 NMP Project NAMDIATREAM (Contract No. 246479), MULTIFUN (Contract No. 262943), ESF PLASMONBIONANOSENSE (Contract No. 5431), EPSRC Active Plasmonics Programme and by Mega-grant from the government of Russian Federation (Contract No. 11.G34.31.0050).

Supporting Information Available: A detailed explanation of optical charateristics of sdAbs–QD and mAbs–AF conjugates; optical characteristics of sdAbs–QD and mAbs–AF conjugates, a table and description representing HER2 expression status of cell models used; concentration curves of HER2 protein labeling in BT-474 and MDA-MB-231 cells models generated by carrying out flow cytometry analysis in order to find optimum concentration of conjugates to be used and brief explanation of this; percentage of cell death upon incubation of MDA-MB-231 with a range of concentrations of sdAbs–QD conjugates used in this study; cytotoxicity assay results of HER2 specific sdAbs–QD and gp120 specific sdAbs–QD in lung and breast cancer cell models; representative flow cytometry histograms of all of the cell models used with all of the conjugates; abbreviations. This material is available free of charge *via* the Internet at http://pubs.acs.org.

REFERENCES AND NOTES

1. Byrne, S. J.; Corr, S. A.; Rakovich, T. Y.; Gun'ko, Y. K.; Rakovich, Y. P.; Donegan, J. F.; Mitchell, S.; Volkov, Y. Optimisation of the Synthesis and Modification of CdTe Quantum Dots for Enhanced Live Cell Imaging. *J. Mater. Chem.* **2006**, *16*, 2896–2902.
2. Rakovich, A.; Rakovich, T.; Kelly, V.; Lesnyak, V.; Eychmüller, A.; Rakovich, Y. P.; Donegan, J. F. Photosensitizer Methylene Blue-Semiconductor Nanocrystals Hybrid System for Photodynamic Therapy. *J. Nanosci. Nanotechnol.* **2010**, *10*, 2656–2662.
3. Rakovich, A.; Savateeva, D.; Rakovich, T.; Donegan, J. F.; Rakovich, Y. P.; Kelly, V.; Lesnyak, V.; Eychmüller, A. CdTe Quantum Dot/Dye Hybrid System as Photosensitizer for Photodynamic Therapy. *Nanoscale Res. Lett.* **2010**, *5*, 753–760.
4. Rousserie, G.; Sukhanova, A.; Even-Desrumeaux, K.; Fleury, F.; Chames, P.; Baty, D.; Oleinikov, V.; Pluot, M.; Cohen, J. H. M.; Nabiev, I. Semiconductor Quantum Dots for Multiplexed Bio-Detection on Solid-State Microarrays. *Crit. Rev. Oncol. Hematol.* **2010**, *74*, 1–15.
5. Sukhanova, A.; Nabiev, I. Fluorescent Nanocrystal-Encoded Microbeads for Multiplexed Cancer Imaging and Diagnosis. *Crit. Rev. Oncol. Hematol.* **2008**, *68*, 39–59.
6. Shi, C.; Zhou, G.; Zhu, Y.; Su, Y.; Cheng, T.; Zhau, H. E.; Chung, L. W. K. Quantum Dots-Based Multiplexed Immunohistochemistry of Protein Expression in Human Prostate Cancer Cells. *Eur. J. Histochem. 52*, 127–134.
7. Tan, A.; Yildirimer, L.; Rajadas, J.; De La Peña, H.; Pastorin, G.; Seifalian, A. Quantum Dots and Carbon Nanotubes in Oncology: A Review on Emerging Theranostic Applications in Nanomedicine. *Nanomedicine (London, U. K.)* **2011**, *6*, 1101–1114.
8. Xing, Y.; Rao, J. Quantum Dot Bioconjugates for *in Vitro* Diagnostics & *in Vivo* Imaging. *Cancer Biomark.* **2008**, *4*, 307–319.
9. Montenegro, J.-M.; Grazu, V.; Sukhanova, A.; Agarwal, S.; de la Fuente, J. M.; Nabiev, I.; Greiner, A.; Parak, W. J. Controlled Antibody/(Bio-) Conjugation of Inorganic Nanoparticles for Targeted Delivery. *Adv. Drug Delivery Rev.* **2013**, *65*, 677–688.
10. Sukhanova, A.; Even-Desrumeaux, K.; Kisserli, A.; Tabary, T.; Reveil, B.; Millot, J.-M.; Chames, P.; Baty, D.; Artemyev, M.; Oleinikov, V.; *et al.* Oriented Conjugates of Single-Domain Antibodies and Quantum Dots: Toward a New Generation of Ultrasmall Diagnostic Nanoprobes. *Nanomedicine* **2012**, *8*, 516–525.
11. Sukhanova, A.; Devy, J.; Venteo, L.; Kaplan, H.; Artemyev, M.; Oleinikov, V.; Klinov, D.; Pluot, M.; Cohen, J. H. M.; Nabiev, I. Biocompatible Fluorescent Nanocrystals for Immunolabeling of Membrane Proteins and Cells. *Anal. Biochem.* **2004**, *324*, 60–67.
12. Alivisatos, a P.; Gu, W.; Larabell, C. Quantum Dots as Cellular Probes. *Annu. Rev. Biomed. Eng.* **2005**, *7*, 55–76.
13. Chang, Y.-P.; Pinaud, F.; Antelman, J.; Weiss, S. Tracking Bio-Molecules in Live Cells Using Quantum Dots. *J. Biophotonics* **2008**, *1*, 287–298.
14. Chen, C.; Peng, J.; Xia, H.-S.; Yang, G.-F.; Wu, Q.-S.; Chen, L.-D.; Zeng, L.-B.; Zhang, Z.-L.; Pang, D.-W.; Li, Y. Quantum Dots-Based Immunofluorescence Technology for the Quantitative Determination of HER2 Expression in Breast Cancer. *Biomaterials* **2009**, *30*, 2912–2918.
15. Resch-Genger, U.; Grabolle, M.; Cavaliere-Jaricot, S.; Nitschke, R.; Nann, T. Quantum Dots *versus* Organic Dyes as Fluorescent Labels. *Nat. Methods* **2008**, *5*, 763–775.
16. Wagner, M. K.; Li, F.; Li, J.; Li, X.-F.; Le, X. C. Use of Quantum Dots in the Development of Assays for Cancer Biomarkers. *Anal. Bioanal. Chem.* **2010**, *397*, 3213–3224.
17. Michalet, X.; Pinaud, F. F.; Bentolila, L. A.; Tsay, J. M.; Doose, S.; Li, J. J.; Sundaresan, G.; Wu, A. M.; Gambhir, S. S.; Weiss, S. Quantum Dots for Live Cells, *in Vivo* Imaging, and Diagnostics. *Science* **2005**, *307*, 538–544.
18. Pinaud, F.; King, D.; Moore, H.-P.; Weiss, S. Bioactivation and Cell Targeting of Semiconductor CdSe/ZnS Nanocrystals with Phytochelatin-Related Peptides. *J. Am. Chem. Soc.* **2004**, *126*, 6115–6123.
19. Wu, X.; Liu, H.; Liu, J.; Haley, K. N.; Treadway, J. A.; Larson, J. P.; Ge, N.; Peale, F.; Bruchez, M. P. Immunofluorescent Labeling of Cancer Marker Her2 and Other Cellular Targets

with Semiconductor Quantum Dots. *Nat. Biotechnol.* **2003**, *21*, 41–46.
20. Goldman, E. R.; Balighian, E. D.; Mattoussi, H.; Kuno, M. K.; Mauro, J. M.; Tran, P. T.; Anderson, G. P. Avidin: A Natural Bridge for Quantum Dot-Antibody Conjugates. *J. Am. Chem. Soc.* **2002**, *124*, 6378–6382.
21. Tokumasu, F.; Dvorak, J. Development and Application of Quantum Dots for Immunocytochemistry of Human Erythrocytes. *J. Microsc.* **2003**, *211*, 256–261.
22. Invitrogen. Quantum Dots & Microspheres http://www.lifetechnologies.com/ie/en/home/life-science/cell-analysis/qdots-microspheres-nanospheres.html (accessed Apr 4, 2014).
23. Howarth, M.; Takao, K.; Hayashi, Y.; Ting, A. Y. Targeting Quantum Dots to Surface Proteins in Living Cells with Biotin Ligase. *Proc. Natl. Acad. Sci. U.S.A.* **2005**, *102*, 7583–7588.
24. Zhou, M.; Ghosh, I. Quantum Dots and Peptides: A Bright Future Together. *Biopolymers* **2007**, *88*, 325–339.
25. Sukhanova, A.; Venteo, L.; Devy, J.; Artemyev, M.; Oleinikov, V.; Pluot, M.; Nabiev, I. Highly Stable Fluorescent Nanocrystals as a Novel Class of Labels for Immunohistochemical Analysis of Paraffin-Embedded Tissue Sections. *Lab. Invest.* **2002**, *82*, 1259–1261.
26. Shemetov, A. A.; Nabiev, I.; Sukhanova, A. Molecular Interaction of Proteins and Peptides with Nanoparticles. *ACS Nano* **2012**, *6*, 4585–4602.
27. Bentolila, L. A. Direct *in Situ* Hybridization with Oligonucleotide Functionalized Quantum Dot Probes. *Methods Mol. Biol.* **2010**, *659*, 147–163.
28. Han, H.; Zylstra, J.; Maye, M. M. Direct Attachment of Oligonucleotides to Quantum Dot Interfaces. *Chem. Mater.* **2011**, *23*, 4975–4981.
29. Clarke, S.; Pinaud, F.; Beutel, O.; You, C.; Piehler, J.; Dahan, M. Covalent Monofunctionalization of Peptide-Coated Quantum Dots for Single-Molecule Assays. *Nano Lett.* **2010**, *10*, 2147–2154.
30. Nabiev, I.; Sukhanova, A.; Artemyev, M.; Oleinikov, V. Fluorescent Colloidal Particles as Detection Tools in Biotechnology Systems. In *Colloidal Nanoparticles in Biotechnology*; John Wiley & Sons, Inc.: Hoboken, NJ, 2007; pp 133−168.
31. Xing, Y.; Chaudry, Q.; Shen, C.; Kong, K. Y.; Zhau, H. E.; Chung, L. W.; Petros, J. A.; O'Regan, R. M.; Yezhelyev, M. V.; Simons, J. W.; *et al.* Bioconjugated Quantum Dots for Multiplexed and Quantitative Immunohistochemistry. *Nat. Protoc.* **2007**, *2*, 1152–1165.
32. Zaman, M. B.; Baral, T. N.; Zhang, J.; Whitfield, D.; Yu, K. Single-Domain Antibody Functionalized CdSe/ZnS Quantum Dots for Cellular Imaging of Cancer Cells. *J. Phys. Chem. C* **2009**, *113*, 496–499.
33. Sukhanova, A.; Even-Desrumeaux, K.; Chames, P.; Baty, D.; Artemyev, M.; Oleinikov, V.; Nabiev, I. Engineering of Ultra-Small Diagnostic Nanoprobes through Oriented Conjugation of Single-Domain Antibodies and Quantum Dots. *Nat. Protoc. Exch.* **2012**, DOI: 10.1038/protex.2012.042; www.nature.com/protocolexchange/protocols/2463.
34. Hamers-Casterman, C.; Atarhouch, T.; Muyldermans, S.; Robinson, G.; Hamers, C.; Songa, E. B.; Bendahman, N.; Hamers, R. Naturally Occurring Antibodies Devoid of Light Chains. *Nature* **1993**, *363*, 446–448.
35. Harmsen, M. M.; De Haard, H. J. Properties, Production, and Applications of Camelid Single-Domain Antibody Fragments. *Appl. Microbiol. Biotechnol.* **2007**, *77*, 13–22.
36. Matz, J.; Kessler, P.; Bouchet, J.; Combes, O.; Ramos, O. H. P.; Barin, F.; Baty, D.; Martin, L.; Benichou, S.; Chames, P. Straightforward Selection of Broadly Neutralizing Single-Domain Antibodies Targeting the Conserved CD4 and Coreceptor Binding Sites of HIV-1 gp120. *J. Virol.* **2013**, *87*, 1137–1149.
37. Even-Desrumeaux, K.; Baty, D.; Chames, P. Strong and Oriented Immobilization of Single Domain Antibodies from Crude Bacterial Lysates for High-Throughput Compatible Cost-Effective Antibody Array Generation. *Mol. BioSyst.* **2010**, *6*, 2241–2248.
38. Saerens, D.; Kinne, J.; Bosmans, E.; Wernery, U.; Muyldermans, S.; Conrath, K. Single Domain Antibodies Derived from Dromedary Lymph Node and Peripheral Blood Lymphocytes Sensing Conformational Variants of Prostate-Specific Antigen. *J. Biol. Chem.* **2004**, *279*, 51965–51972.
39. Even-Desrumeaux, K.; Fourquet, P.; Secq, V.; Baty, D.; Chames, P. Single-Domain Antibodies: A Versatile and Rich Source of Binders for Breast Cancer Diagnostic Approaches. *Mol. BioSyst.* **2012**, *8*, 2385–2394.
40. Even-Desrumeaux, K.; Nevoltris, D.; Lavaut, M. N.; Alim, K.; Borg, J.-P.; Audebert, S.; Kerfelec, B.; Baty, D.; Chames, P. Masked Selection: A Straightforward and Flexible Approach for the Selection of Binders against Specific Epitopes and Differentially Expressed Proteins by Phage Display. *Mol. Cell. Proteomics* **2014**, *13*, 653–665.
41. Santin, A. D.; Bellone, S.; Roman, J. J.; McKenney, J. K.; Pecorelli, S. Trastuzumab Treatment in Patients with Advanced or Recurrent Endometrial Carcinoma Overexpressing HER2/neu. *Int. J. Gynaecol. Obstet.* **2008**, *102*, 128–131.
42. Jacobs, T. W.; Gown, A. M.; Yaziji, H.; Barnes, M. J.; Schnitt, S. J. Specificity of HercepTest in Determining HER-2/neu Status of Breast Cancers Using the United States Food and Drug Administration-Approved Scoring System. *J. Clin. Oncol.* **1999**, *17*, 1983–1987.
43. Figueroa-Magalhães, M. C.; Jelovac, D.; Connolly, R. M.; Wolff, A. C. Treatment of HER2-Positive Breast Cancer. *Breast* **2014**, *23*, 128–136.
44. Jelovac, D.; Emens, L. A. HER2-Directed Therapy for Metastatic Breast Cancer. *Oncology* **2013**, *27*, 166–175.
45. Hanna, W.; Barnes, P.; Berendt, R.; Chang, M.; Magliocco, A.; Mulligan, A. M.; Rees, H.; Miller, N.; Elavathil, L.; Gilks, B.; *et al.* Testing for HER2 in Breast Cancer: Current Pathology Challenges Faced in Canada. *Curr. Oncol.* **2012**, *19*, 315–323.
46. Tan, M.; Yu, D. Molecular Mechanisms of erbB2-Mediated Breast Cancer Chemoresistance. *Adv. Exp. Med. Biol.* **2007**, *608*, 119–129.
47. Ross, J. S.; Fletcher, J. A. The HER-2/neu Oncogene in Breast Cancer: Prognostic Factor, Predictive Factor, and Target for Therapy. *Stem Cells* **1998**, *16*, 413–428.
48. Lidke, D. S.; Nagy, P.; Heintzmann, R.; Arndt-Jovin, D. J.; Post, J. N.; Grecco, H. E.; Jares-Erijman, E. A.; Jovin, T. M. Quantum Dot Ligands Provide New Insights into erbB/HER Receptor-Mediated Signal Transduction. *Nat. Biotechnol.* **2004**, *22*, 198–203.
49. Shih, J.; Yuan, A.; Chen, J.; Yang, P. Tumor-Associated Macrophage: Its Role in Cancer Invasion and Metastasis. *J. Cancer Mol.* **2006**, *2*, 101–106.
50. Yarden, Y.; Sliwkowski, M. X. Untangling the ErbB Signalling Network. *Nat. Rev. Mol. Cell Biol.* **2001**, *2*, 127–137.
51. Baselga, J.; Swain, S. M. Novel Anticancer Targets: Revisiting ERBB2 and Discovering ERBB3. *Nat. Rev. Cancer* **2009**, *9*, 463–475.
52. Ciardiello, F.; Tortora, G. A Novel Approach in the Treatment of Cancer: Targeting the Epidermal Growth Factor Receptor. *Clin. Cancer Res.* **2001**, *7*, 2958–2970.
53. Mendelsohn, J.; Baselga, J. The EGF Receptor Family as Targets for Cancer Therapy. *Oncogene* **2000**, *19*, 6550–6565.
54. Slamon, D. J.; Godolphin, W.; Jones, L. A.; Holt, J. A.; Wong, S. G.; Keith, D. E.; Levin, W. J.; Stuart, S. G.; Udove, J.; Ullrich, A. Studies of the HER-2/neu Proto-Oncogene in Human Breast and Ovarian Cancer. *Science* **1989**, *244*, 707–712.
55. Paik, S.; Hazan, R.; Fisher, E. R.; Sass, R. E.; Fisher, B.; Redmond, C.; Schlessinger, J.; Lippman, M. E.; King, C. R. Pathologic Findings from the National Surgical Adjuvant Breast and Bowel Project: Prognostic Significance of erbB-2 Protein Overexpression in Primary Breast Cancer. *J. Clin. Oncol.* **1990**, *8*, 103–112.
56. Kenfield, S. A.; Wei, E. K.; Stampfer, M. J.; Rosner, B. A.; Colditz, G. A. Comparison of Aspects of Smoking among the Four Histological Types of Lung Cancer. *Tob. Control* **2008**, *17*, 198–204.
57. ATCC: The Global Bioresource Center http://www.lgcstandards-atcc.org/?geo_country=ie (accessed Apr 4, 2014).

58. Abramoff, M.; Magelhaes, P.; Ram, S. Image Processing with ImageJ. *Biophotonics Int.* **2004**, *11*, 36–42.
59. Bunn, P. A.; Helfrich, B.; Soriano, A. F.; Franklin, W. A.; Varella-Garcia, M.; Hirsch, F. R.; Baron, A.; Zeng, C.; Chan, D. C. Expression of Her-2/neu in Human Lung Cancer Cell Lines by Immunohistochemistry and Fluorescence *in Situ* Hybridization and Its Relationship to *in Vitro* Cytotoxicity by Trastuzumab and Chemotherapeutic Agents. *Clin. Cancer Res.* **2001**, *7*, 3239–3250.
60. Tseng, P.-H.; Wang, Y.-C.; Weng, S.-C.; Weng, J.-R.; Chen, C.-S.; Brueggemeier, R. W.; Shapiro, C. L.; Chen, C.-Y.; Dunn, S. E.; Pollak, M.; *et al*. Overcoming Trastuzumab Resistance in HER2-Overexpressing Breast Cancer Cells by Using a Novel Celecoxib-Derived Phosphoinositide-Dependent Kinase-1 Inhibitor. *Mol. Pharmacol.* **2006**, *70*, 1534–1541.
61. Subik, K.; Lee, J.-F.; Baxter, L.; Strzepek, T.; Costello, D.; Crowley, P.; Xing, L.; Hung, M.-C.; Bonfiglio, T.; Hicks, D. G.; *et al*. The Expression Patterns of ER, PR, HER2, CK5/6, EGFR, Ki-67 and AR by Immunohistochemical Analysis in Breast Cancer Cell Lines. *Breast Cancer* **2010**, *4*, 35–41.
62. Yu, W. W.; Qu, L.; Guo, W.; Peng, X. Experimental Determination of the Extinction Coefficient of CdTe, CdSe, and CdS Nanocrystals. *Chem. Mater.* **2003**, *15*, 2854–2860.
63. Niesner, R.; Peker, B.; Schlüsche, P.; Gericke, K.-H. Noniterative Biexponential Fluorescence Lifetime Imaging in the Investigation of Cellular Metabolism by Means of NAD(P)H Autofluorescence. *ChemPhysChem* **2004**, *5*, 1141–1149.
64. Wu, Y.; Lopez, G. P.; Sklar, L. A.; Buranda, T. Spectroscopic Characterization of Streptavidin Functionalized Quantum Dots. *Anal. Biochem.* **2007**, *364*, 193–203.
65. Medintz, I. L.; Stewart, M. H.; Trammell, S. A.; Susumu, K.; Delehanty, J. B.; Mei, B. C.; Melinger, J. S.; Blanco-Canosa, J. B.; Dawson, P. E.; Mattoussi, H. Quantum-Dot/Dopamine Bioconjugates Function as Redox Coupled Assemblies for *in Vitro* and Intracellular pH Sensing. *Nat. Mater.* **2010**, *9*, 676–684.
66. Holliger, P.; Hudson, P. J. Engineered Antibody Fragments and the Rise of Single Domains. *Nat. Biotechnol.* **2005**, *23*, 1126–1136.